Performance of MEMS-Based Gas Distribution and Control Systems for Semiconductor Processing

Albert K. Henning [a], John Fitch[b] , James M. Harris, Errol B. Arkilic, Brad Cozad, and Ben Dehan

Redwood Microsystems, Inc., 959 Hamilton Avenue, Menlo Park, CA 94025

ABSTRACT

The advent of microelectromechanical systems has enabled dramatic changes in diverse technological areas. In terms of control and distribution of liquids and gases (microfluidics), MEMS-based devices offer opportunities to achieve increased performance, and higher levels of functional integration, at lower cost, with decreased size and increased reliability. This work focuses on recent research and development of high-purity gas distribution and control systems for semiconductor processing. These systems include the following components, based upon both normally-open and normally-closed microvalves: pressure-based mass flow controllers; vacuum leak-rate shut-off valves; and pressure regulators. Advanced packaging techniques enable these components to be integrated into gas sticks and panels which have small size, corrosion-resistant wetted materials, small dead volumes, and minimal particle generation. Principles of operation of components and panels, and performance data at both the component and system level, will be presented. The potential for 10x size reduction (linear dimension), 2x product yield improvement (through increased reliability, improved flow accuracy and repeatability, and contamination reduction), and 5x reduction in process gas consumption, will also be addressed. Particular emphasis on characterization and verification of flow measurements in mass flow controllers (versus NIST standards), and the flow models used in designing and characterizing these systems, will be made.

Keywords: MEMS, microvalve, microfluidics, mass flow control

LIST OF VARIABLES

dV_F, V_o	Volumetric change and initial volume of Fluorinert liquid
b	Temperature coefficient of expansion of Fluorinert liquid
T_{FC}, T_{fill}	Mean and fill temperatures of Fluorinert liquid
s, z, a	Membrane stroke, membrane-to-NO-orifice gap, and membrane radius
h, t	Membrane, cavity thickness
P	Pressure differential across the membrane
E, m	Young's modulus (190,000 MPa) and Poisson's ratio (0.09) for silicon
$\dot{m}$	Mass flow (usually in sccm, normalized to 273 K and 1 atm)
$Power_{in}$	Microvalve inlet power (=VI)
P_{in}	Inlet pressure
P_{out}	Outlet pressure
P_x, P_{sense}	Intermediate (pressure sensor) pressure
g	Ratio of specific heats, c_p/c_v
a	$= \sqrt{g\left(\frac{2}{1+g}\right)^{\frac{g+1}{g-1}}}$
d	$= \sqrt{\frac{4g}{(g+1)(g-1)}}$
R	Gas constant in $p = rRT$ (8314 m^2/K-sec^2 divided by molecular weight)

[a] Email: henning@redwoodmicro.com; WWW: http://www.redwoodmicro.com; Telephone: 650-617-0854; FAX: 650-326-9217

[b] Present Address: Xerox PARC, Palo Alto, CA; Email: fitch@parc.xerox.com; Telephone: 650-812-4226; FAX: 650-812-4133

r	Gas or Fluorinert liquid density
D (or d)	Orifice diameter
D_h	Hydraulic, or effective, diameter of microvalve flow area
A	Orifice or microvalve flow area
C_d	Orifice or microvalve coefficient of discharge
C_{FC}	Fluorinert liquid specific heat capacity
R_{th}	Lumped thermal microvalve resistance
R_0, T_0	Microvalve resistor valve R_0 at temperature T_0, used to determine TCR
TCR	Microvalve resistor temperature coefficient of resistance (in Ω/K)
E, μ	Young's modulus (1.9×10^{11} Pa), Poisson ratio (0.09) for silicon

1.0 INTRODUCTION

Gas distribution and control systems for semiconductor processing based on microelectromechanical systems (MEMS) are comprised of a variety of components. ***Sensors*** are used to measure fluid properties such as pressure, temperature, and flow. ***Actuators***, primarily valves but possibly including pumps and compressors, are used to alter the state of the fluid pressure, temperature, or flow. ***Distribution channels***, such as orifices and microchannels, carry the fluid from one portion of the system to another. A crucial aspect is the requirement for ***systems integration*** of microfabricated components. Electronics, control algorithms, materials compatibility in the fluidic wetted path, packaging, and system testing are critical to the achievement of a fully functional system. Fabricating only the micro-components of the system is never sufficient.

Previous work has demonstrated the development of thermopneumatically-actuated microvalves.[1] Control of gas flow using other actuation means has been detailed as well.[2] Control of liquids using microvalves has been explored, including the integrated mass flow control of gases and liquids in chemical systems[3] and refrigerant liquids.[4] Some recent work also explored mass flow controllers built using microfabrication techniques.[5] Lately, the incorporation of microfabricated components into gas control systems for semiconductor processing has begun. Some initial theory and results have been presented,[6] and the importance of packaging has been emphasized.[7]

This work extends the results of previous work.[6,7] X-ray tomographic images of the vacuum leak-rate shut-off valve are shown. Increased accuracy and resolution of mass flow controllers are presented, along with a more detailed theoretical foundation for the design and analysis of these devices. A brief review of the various components of MEMS-based gas distribution systems is first made. Then, the theory and modeling underlying the design and characterization and analysis of vacuum leak-rate shut-off valves, and mass-flow controllers, are presented. Recent results, especially in the systems-level modeling of mass flow controller behavior (as opposed to the component-level modeling of previous work), are given. Finally, conclusions and expectations for further improvements are made.

2.0 HIERARCHY OF COMPONENT AND SYSTEM TECHNOLOGY

MEMS-based components may be used to create devices with higher levels of functionality, appropriate for use in the control and distribution of gases for semiconductor device processing. This section outlines these components.

2.1 Normally-closed shut-off valves.

Normally-closed (NC) microvalves are important components of MEMS-based devices such as gas sticks. We have created NC valve modules which have a wetted path composed entirely of nickel or ceramic (Al_2O_3), and silicon. These valves also have incorporated a proprietary sealing technology, which enables very low leak rates to be obtained.[6] As with the normally-open (NO) microvalve used in mass-flow control (MFC) or pressure regulator (PR) modules (see Section 2.4), wetted surfaces may be coated with SiC or Si_3N_4, in order to provide materials compatibility in situations where a wetted silicon surface would be undesirable.

Figure 1 shows a cross-section of this NC, low-leakage shut-off valve. The thermopneumatic actuation principle[1] is employed. A silicon cantilever is either fusion- or epoxy-bonded to the boss on the membrane. Under conditions of zero input power, this cantilever provides the shut-off property by sealing against a low-leakage seat (polished silicon). As

shown, the wetted path is entirely silicon and nickel or ceramic. The microvalve is bonded to the nickel or ceramic using either a eutectic bond, or a PTFE (Teflon™) based die attach material. An x-ray tomographic image of a finished NC vacuum leak-rate shut-off microvalve is shown in the lower portion of Figure 1. Note the 'S'-shape of the membrane, produced by the pull-in force due to the thermopneumatic liquid, and the contact force between the O-ring and the valve seat. The overall dimensions are 8 mm x 6 mm x 2 mm. Results are given in Section 3.1.

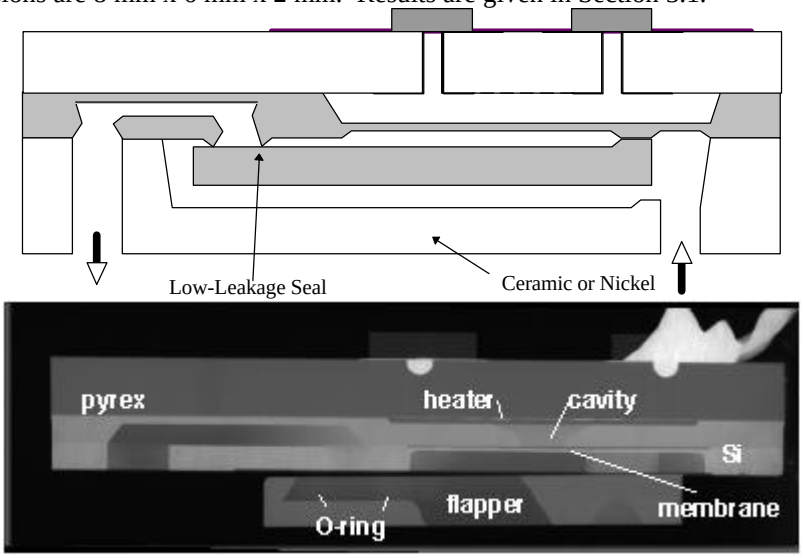

Figure 1*: Upper: Cross-section schematic of a thermopneumatically-actuated, normally-closed, vacuum leak-rate, shut-off microvalve. Lower: X-ray tomographic image of an actual valve.*

2.2 Normally-open proportional control valves.

Normally-open (NO) proportional control valves using thermopneumatic actuation have been reported since 1986.[8] Figure 2 shows a cross-section of an NO proportional control valve. The fabrication process has been described elsewhere,[1] but relies on both silicon fusion bonding,[9] and silicon-to-Pyrex anodic bonding.[10] Since the valve is surface mounted, no Pyrex is exposed to the fluid traversing the valve. Typical dimensions are: 6.0 x 6.3 mm^2 lateral dimension; 0.8 mm thick Pyrex; 0.4 mm thick membrane layer, with 50 mm thick membrane; 0.4 mm thick orifice layer; 25-500 μm orifice.

The thermopneumatic actuation principle relies on a hermetically sealed cavity, which is filled with Fluorinert™ (FC). The cavity incorporates a platinum resistor, to provide controlled heat transfer to the FC liquid. The cavity is rigid on five of its six sides. The sixth side is comprised of a flexible, single-crystal silicon membrane. Heating the FC liquid causes it to expand. The membrane moves in response to this expansion, and ultimately forms a seal with the valve seat, which is also comprised of silicon.

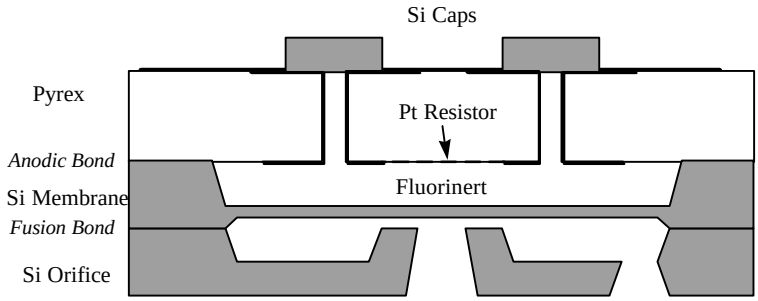

Figure 2*: Cross-section of a thermopneumatically-actuated, normally-open, proportional control microvalve.*

2.3 Sensors and Flow Distribution Elements.

In creating devices with higher levels of functionality, small (several millimeters square) temperature sensors and piezoresistive pressure sensors are used to monitor temperature and pressure in the device flow path. These sensors are

commercially available. When incorporated into, for instance, a final flow control device, the information they provide becomes the basis for the calibration data (stored on E^2PROM) connecting reported flow to measured pressure and temperature, using the flow models shown in Section 3. It is important that sensing occur as close as possible to the flow point of interest. For instance, in a low-flow MFC, the pressure must be sensed as close as possible to the inlet of the critical orifice.

The distribution of flow requires careful consideration. Channels in silicon, as well as micromachined orifices (see Figure 3) and passages through packages and manifolds, must meet the requirements of low or no pressure drop, and maintenance of laminar or other designed flow conditions, with no impact on system reliability. For purposes of this work, at the intended fluid working pressures and flows, and using the structures described, these conditions are met easily using silicon, alumina, or nickel. These materials have very smooth surfaces in terms of particle generation, are reasonably well matched in terms of coefficient of thermal expansion, and are large compared to most of the hydraulic dimensions in these devices. An exception occurs for the critical flow orifice described in the next section. This element, along with the microvalve, has the smallest hydraulic dimension in a pressure-based MFC. As such, it affects the pressure vs. flow relationship in the system at the most fundamental level.

2.4 Higher-order systems: mass-flow controllers and pressure regulators.

Higher-order systems can be created from these components. For instance, Figure 3 shows a schematic cross-section of a mass-flow controller. This device has been described in detail elsewhere, and will be reviewed in Section 3. Briefly, it works according to the following principles. Flow through an orifice which exceeds the speed of sound is called critical flow, and is described mathematically by an expression which is linearly proportional to the pressure upstream of the orifice. This relationship enables a model equation to relate MFC flow and pressure sensed upstream of the orifice. This flow is compared to a set point flow. Depending upon the relationship between measured and set point flows, the valve is throttled either up or down, to increase or decrease the pressure upstream of the orifice. A pressure regulator is constructed identically to the MFC, except that the orifice is removed, and closed loop feedback occurs directly between the pressure sensor and the microvalve, without a flow model as the intermediary.

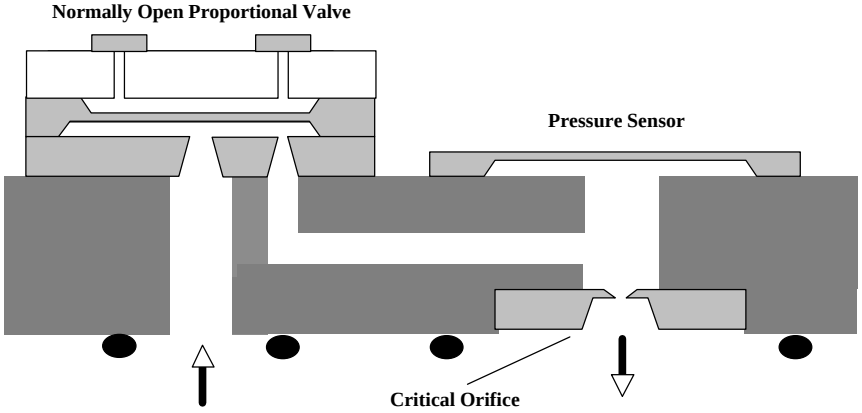

***Figure 3**: Cross-section of a mass flow controller. Not shown are the temperature sensor, second pressure sensor, and E^2PROM. A pressure-regulator is created by removing the critical flow orifice from the device shown here. The silicon components are mounted onto a substrate comprised of either alumina (ceramic) or nickel.*

2.5 Higher-order systems: gas panels.

Higher-order systems can be created from MFCs, PRs, and shut-off valves. In particular, gas 'sticks', and multiple-channel gas panels, much smaller than otherwise available, can be made. Figure 4 shows two such integrated gas distribution systems. The first photo shows a four-channel gas panel. Each channel consists of inlet and outlet shut-off valves, a PR, and an MFC with a purge line connection (both not shown, on panel back). The panel has an additional purge line (accessed by the single shut-off module in the top of the photo). The panel dimensions are approximately 150 mm x 100 mm x 25 mm. The second photo shows a prototype of a revolutionary gas stick. In this example, a single gas control

channel is comprised of inlet and outlet shut-off valves, a purge-line shut-off valve connection, and an MFC. The components are all mounted on a ceramic manifold. The square microvalve is 6 mm square, as a reference dimension.

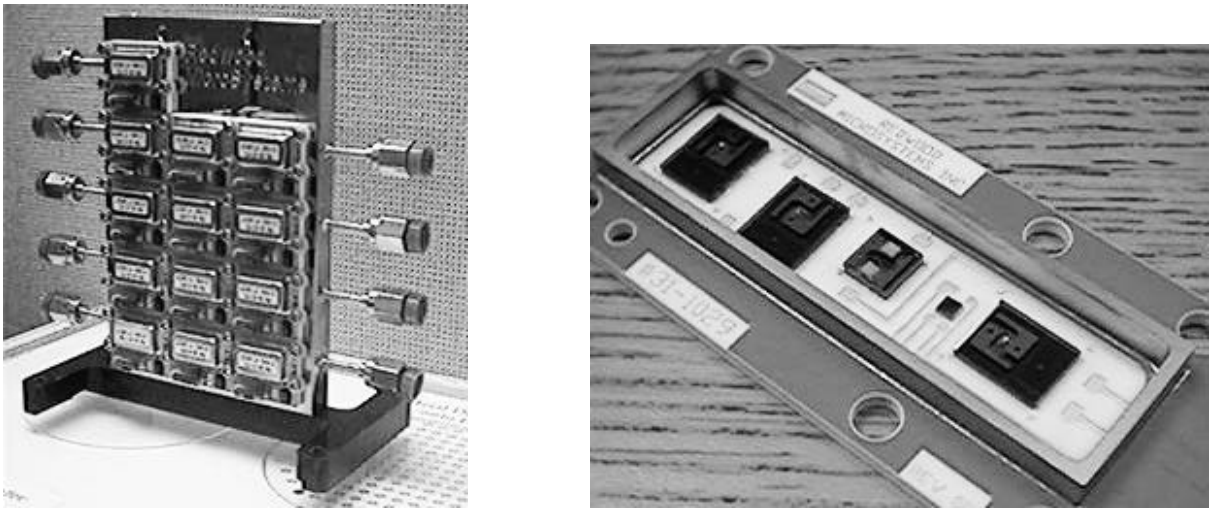

***Figure 4**: Photographs of integrated gas distribution systems. Left: A four-channel gas panel with a purge line. Right: A prototype of the next-generation gas stick.*

3.0 CALCULATION DETAILS

3.1 Normally-closed shut-off valves.

Figure 5 shows the schematic cross-section of the sealing interface between an elastomer (O-ring) and the polished silicon valve seat. The sealing force compresses the elastomer, as depicted. Approximately, the leak rate through the elastomer, as a function of pressure drop, gas diffusion coefficient *k* for the elastomer, and O-ring geometry, is:

$$\dot{m}_{leak} \equiv 2pR \cdot \Delta P \cdot k \cdot 2 \int_0^{y_{\max}} \frac{dy}{2\sqrt{r^2 - y^2}} \tag{1}$$

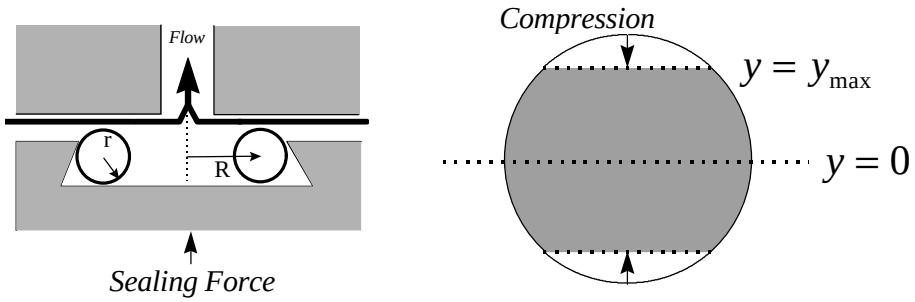

***Figure 5**: Schematic of O-ring used in the vacuum leak-rate shut-off valve calculations.*

Calculations based on Equation (1) encouraged the design and fabrication of the vacuum leak-rate NC valves. Results from measurements will be shown in Section 4.

3.2 Normally-open proportional control valves.

Development of a functional relationship between microvalve signal input, and flow response, is fundamental to most of the microfluidics devices under consideration in this work. In this section, previous details of such a model between system inputs and outputs are recapitulated and extended. The goal of a model relating inputs to outputs for thermopneumatically actuated microvalves must connect input power to output flow, with external temperature and pressure boundary conditions serving as secondary inputs. For gases, the compressible flow equations for subsonic and sonic flow are given in

Equation (2).[11] Sonic flow occurs only rarely in the microvalves used in our gas distribution systems, so that we focus on the lefthand portion of Equation (2). Based on this subsonic, compressible flow model, we must relate the modeled flow area to the empirical or effective flow area, which is a function of the gap between the membrane and the flow inlet.

$$\dot{m}_{subsonic} = \frac{P_{in}}{\sqrt{RT}} C_d A \left(\frac{P_{out}}{P_{in}}\right)^{1/g} d(g) \sqrt{\left(\frac{P_{in}}{P_{out}}\right)^{\frac{g-1}{g}} - 1} \qquad \dot{m}_{sonic} = P_{in} C_d A \frac{a(g)}{\sqrt{RT}} \tag{2a,b}$$

Figure 6 shows a schematic representation of this gap *z-s*. *z* is the equilibrium distance between the membrane and the flow inlet, while *s* is the deflection of the membrane from its equilibrium position, sometime called the stroke. Earlier details of the NO device behavior may be found.[1,6] The behavior of single-crystal silicon membranes has also been described,[12] providing a relationship between the membrane stroke and the transmembrane pressure, shown in Equation (3). This pressure is the difference between the pressure in the hermetically sealed, thermopneumatic cavity, and the external pressure. Simultaneously, the membrane stroke is also related to the mean temperature of the Fluorinert liquid, as shown in Equation (4). Changes in the volume of this liquid are proportional to the mean liquid temperature in excess of the temperature at which the cavity is filled. Volume change must be translated into membrane stroke; Equation (4) gives this volume-stroke relationship for a circular membrane of radius *a*. These expressions hold for liquid-only phase in the thermopneumatic cavity. The effects of liquid-gas phase changes on membrane behavior are given elsewhere.[13]

$$s = 0.0151 \cdot (1 - m^2) \cdot \frac{Pa^4}{Eh^3} \tag{3}$$

$$dV_F = V_0 \cdot b \cdot (T_{FC} - T_{fill}) \qquad dV_F = \frac{1}{6} ps(3a^2 + s^2) \tag{4a,b}$$

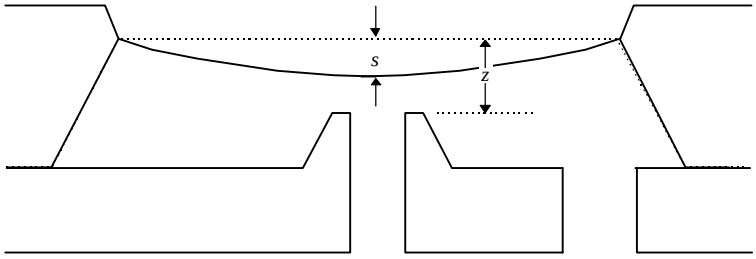

***Figure 6**: Relationship between the equilibrium membrane-to-inlet distance z and the stroke s.*

Extracting the effective diameter ($=\sqrt{A}$) for a microvalve, and completing a quantitative model according to Equations (2), can only be done via experimental characterization of fabricated microvalves. For the types of devices represented by Figure 2, with or without a membrane boss, Equation (5) holds for subsonic flow conditions, in microvalves with maximum flows ranging from 1 to 2000 sccm, and with equilibrium gaps *z* ranging from 10 to 50 µm.

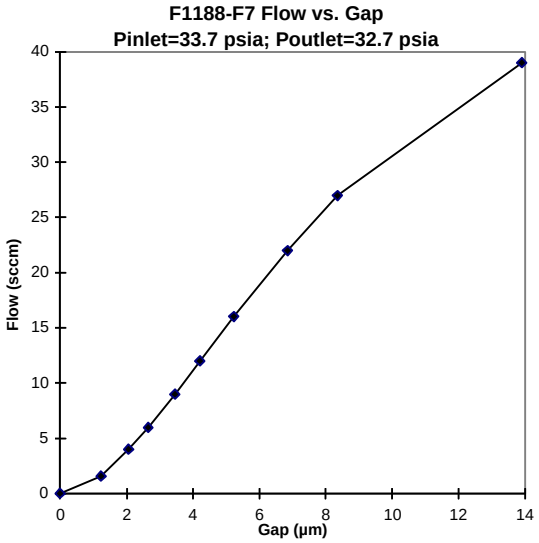

***Figure 7**: Measured flow versus gap z-s for a normally-open microvalve. The predicted curve differs by less than 2% over the range of the gap parameter.*

Unlike the loss coefficient model for the effective valve area reported earlier,[6] we have subsequently related this effective area to the inlet diameter D_{inlet}, and the ratio of the equilibrium gap to this inlet diameter. Figure 7 shows an example of measured flow versus membrane-to-inlet gap *z*-*s*. The predicted values using Equation (5) differ from the measured values by less than 2% over the range of the gap. This measured curve was derived from separately measured flow versus power, and gap versus power, curves. Note that the function $D_h(D_{inlet}, \frac{z-s}{D_{inlet}})$ used in Equation (5) also holds for an expression of sonic flow through a microvalve. This sonic flow expression is given by substituting *A* in Equation (2b) by D_h^2. Since they will vary for other microvalve structures, the functional details of D_h are not included in this work.

$$\dot{m}_{NO} = \frac{P_{in}}{\sqrt{RT}} C_d D_h^2(D_{inlet}, \tfrac{z-s}{D_{inlet}}) \left(\frac{P_{out}}{P_{in}}\right)^{1/g} d\sqrt{\left(\frac{P_{in}}{P_{out}}\right)^{\frac{g-1}{g}} - 1} \tag{5}$$

The response time of a NO microvalve can be estimated using Equations (6)-(8). Equation (6) shows a lumped-element, transient response equation for the NO microvalve system. It assumes all energy is stored in the Fluorinert liquid, and lumps the effective thermal resistance into a single parameter. In steady-state, this expression reduces to Equation (7a). The platinum resistor has a well-defined temperature coefficient of resistance. This relationship can be used to relate the effective thermal resistance of the microvalve, to the power input *VI* to the microvalve, as shown in Equation (7b). Together, Equations (7) allow derivation of effective thermal resistance and mean Fluorinert temperature from measurements of microvalve input power and ambient temperature.

$$rV_0C_{FC}\frac{dT_{FC}}{dt} = Power_{in} - \frac{T_{FC} - T_{ambient}}{R_{th}} \tag{6}$$

$$T_{FC,ss} = Power_{in}R_{th} + T_{ambient} \qquad R_{th} = \frac{T_0 - T_a + \left(\frac{V}{I} - R_0\right)\Big/TCR}{VI} \tag{7a,b}$$

We can then use Equation (4) and Equation (6) together to look at the full transient behavior of the microvalve in going from an unpowered to a powered state. We can assume all the energy input goes into the FC liquid, and is not lost to the surroundings, in order to estimate the minimum rise time of the microvalve. Then, the time associated with deflecting the membrane an amount *s* is:

$$t_{rise,\min} = \frac{rC_{FC}}{b}\frac{1}{Power_{in}}\frac{1}{6}ps(3a^2 + s^2) \tag{8}$$

So, if the thermopneumatic cavity is completely filled with liquid (hydraulically locked), then the Fluorinert liquid's material parameters, the power input, and the differential volume of the expanded liquid, control fully the estimate of rise time. For a microvalve with a 50 μm stroke (to close the valve), 2 mm membrane radius, and a power input of 1 W, the time required to close the valve from its equilibrium position is estimated to be 0.37 sec or greater. This compares well to observed values ranging from 0.5 to 1.0 sec. Note that Equation (8) also leads readily to estimates of the effect of scaling on thermopneumatic microvalve response times.

3.3 Sensors and Flow Distribution Elements.

The flow resolution of a pressure-based MFC depends completely upon the pressure resolution of the pressure sensors, and the sonic, compressible flow of gas through the orifice. Taking the derivative of Equation (2) creates a relationship between flow resolution and pressure sensor resolution, for sonic flow through a critical orifice. Figure 8 plots this derivative expression, as a function of critical orifice diameter, using C_d=1. As an example of the use of Figure 8, consider the case where an available pressure sensor has a resolution of 0.1 psid, and the desired flow resolution is 0.01 sccm. Then the diameter of the critical orifice must exceed 10 μm. So, the orifice size sets not only the gas flow rate, but also the flow resolution. As is also apparent, the pressure sensors are crucial to the function of pressure-based MFCs and pressure regulators. Long-term sensor drift must be considered, in order to deliver the highest performance device.

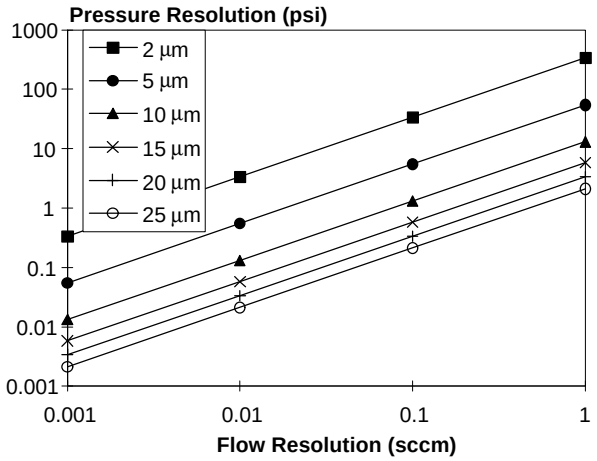

Figure 8*: Pressure resolution required to deliver a given flow resolution, as a function of critical orifice diameter.*

3.4 Higher-order systems: mass-flow controllers and pressure regulators.

The compressible gas flow expressions in Equations (2) can be used to represent the critical orifice and microvalve flow elements of an MFC. In addition, Equations (3), (4), and (7) can be used to derive a relationship between valve input power, and membrane stroke. Using these expressions together, a model for the flow as a function of the input valve voltage or power can be constructed. Figure 9 shows a schematic representation of the series combination of an NO microvalve and a critical orifice (CO) which constitutes the MFC. The inlet and outlet pressures for the MFC are also shown. The outlet pressure for the NO microvalve is P_x, while the inlet pressure for the CO is also P_x. The ratio of the inlet and outlet pressures for each flow element determines whether to use the sonic or subsonic expression in Equations (2) to model the flow through that element. Roughly speaking, if $P_{in} / P_x > 2$, then the flow through the NO is sonic. Similarly, if $P_x / P_{out} > 2$, then the flow through the CO is sonic. This ratio changes, depending upon the gas which acts as the MFC's working fluid.[11] Once the appropriate flow equation for each device is determined, the two equations are set equal to each other, and P_x is found. This process is shown schematically in Figure 10. In this example, the MFC inlet pressure is 50 psia, and the outlet pressure is 200 Torr. The CO, being a passive fluidic element, has a single curve, while the NO microvalve acquires a different characteristic curve, depending upon the position *z-s* between the membrane and the valve inlet. The intersection of the two curves, for given values of inlet and outlet pressure, and of *z-s*, is the solution for P_x. It also gives the result for the steady-state flow. Figure 10 also shows how the values of flow and intermediate pressure decrease, as the value of *z-s* decreases (or, as the power input to the valve increases). In this modeled example, both the microvalve and the CO have coefficients of discharge equal to unity. The CO diameter is 16.5 µm. The microvalve has a gap *z* of 10 µm, and an inlet size of 50 µm.

Figure 11 shows the results of a comparison of this system-level MFC flow model, and an actual MFC. The good agreement between the two provides a solid foundation for further modeling, research, development, and design efforts. The parameters for the device are: C_d (CO)=0.86; C_d (NO)=0.76; inlet diameter (NO)=550 µm; inlet diameter (CO)=90 µm; NO microvalve gap *z*=30 µm. Coefficients of discharge were determined by fits to data from comparable, separate elements. The difference between modeled and measured inlet sizes and gap size were less than five percent.

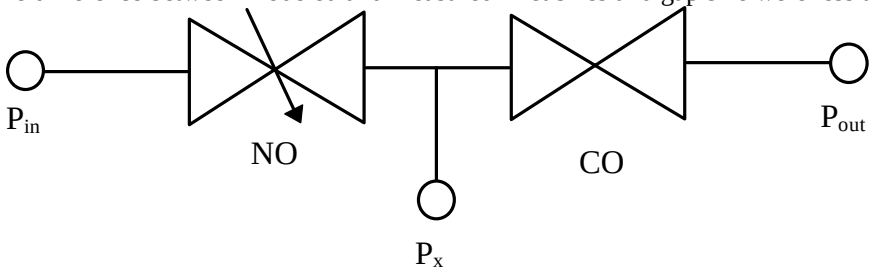

Figure 9*: Schematic representation of the compressible flow model for the series combination of a normally-open proportional valve, and a critical orifice.*

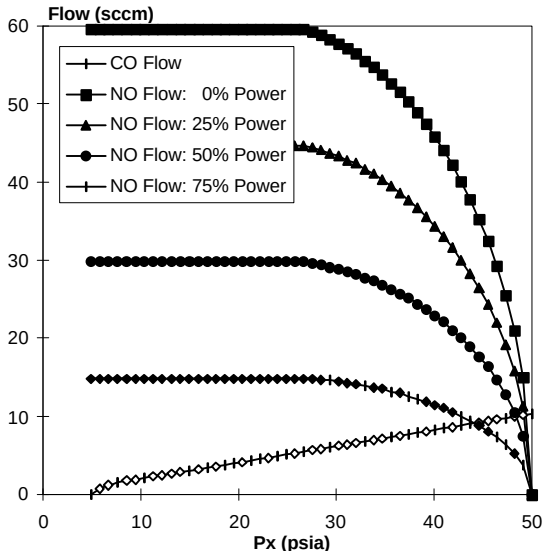

***Figure 10**: Example of the compressible flow model for the MFC.*

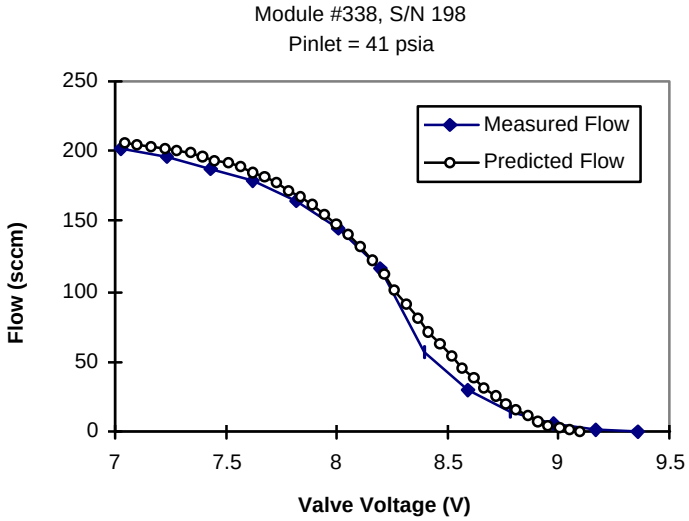

***Figure 11**: Comparison of measurements and modeling of the flow versus valve voltage characteristics for a 200 sccm MFC.*

4.0 RESULTS

4.1 Normally-closed shut-off valves.

Figure 12 shows measured helium leak rates for a set of vacuum leak-rate shut-off NC microvalves, built according to Figure 1. The sealing material in these devices is Viton; characterization of seals made with other materials, such as Kel-F™, has also been accomplished. Also shown is data from a standard shut-off valve commonly used in the industry. The SEMATECH specification for shut-off valves states they must flow less than 10^{-9} cc-He/sec after 15 seconds of full-off actuation. Shut-off valves used at present in the industry reach higher steady-state leak rates than these microvalves, due to their more permeable sealing materials, smaller compression forces on the sealing surfaces, and larger effective leak cross-sections. At the same time, the width of their sealing surfaces is greater than in our microvalve, occasionally resulting in lower metastable values of leak rate.

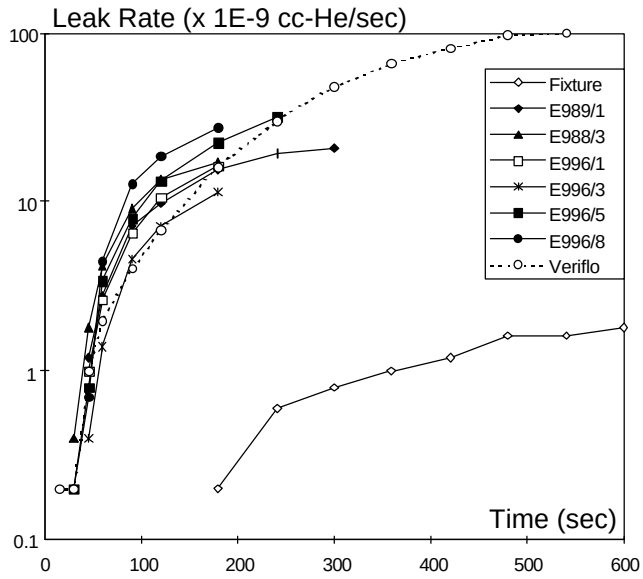

***Figure 12**: Helium leak rates for vacuum leak-rate shut-off microvalves.*

4.2 Normally-open proportional control valves.

Much data of flow versus pressure data has been accumulated, as a function of NO microvalve structural sizes, ambient temperature and pressure, and valve inlet power. Figure 7 was one example of such measurements. Figure 13 shows a further comparison of the modeled and measured flow for a NO microvalve. In this case, the measured valve inlet size was 89 µm, compared to the modeled 87 µm. The measured and modeled gap *z* at room pressure was 16 µm. The coefficient of discharge is 0.75. Departures of the model and measurements are due to fluctuations in the membrane position caused by the variation in outlet pressure.[13] Similar results have been obtained for microvalves with rated maximum flows of nitrogen from 10 sccm to 2000 sccm, with inlet pressures of 20 psig and a 1 psid pressure drop across the valve.

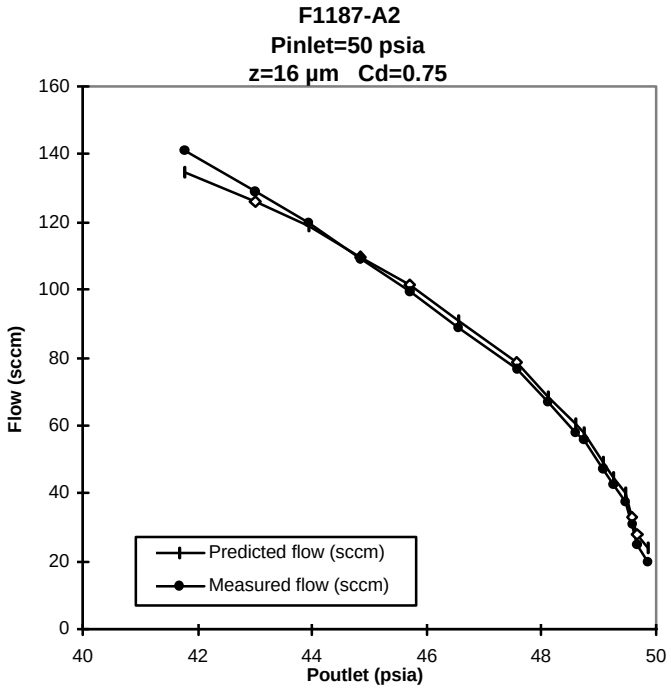

***Figure 13**: Comparison of modeling and measurements of open (unpowered) flow for a NO microvalve.*

4.3 Higher-order systems: mass-flow controllers and pressure regulators.

MEMS-based mass flow controllers provide high resolution and accuracy compared to conventional thermal-based mass flow controllers. For use in semiconductor device processing, such resolution and accuracy are essential to achievement of high process yields and device reliability. Figure 14 shows the results of measured comparisons between MEMS-based, pressure-based MFCs, and thermal-based MFCs. The devices shown have a maximum rated flow of 10 sccm of nitrogen. Similar results have been observed at higher flow rates. The tests were performed according to SEMASPEC #92071221 B-STD. Measurements were performed on a primary flow standard based on rate-of-rise of pressure measurements.[14] Accuracy of better than 1% of reading over a 10:1 dynamic range is the outstanding achievement of these devices. The resolution of better than 0.5% of reading for a 5:1 dynamic range is also significant. The success of these devices is founded on the accuracy, precision, and resolution of readings of pressure in the system. Further improvements are possible through refinements in the empirical characterization of flow as a function of various applied pressures and ambient temperature, especially as they impact stress-induced fluctuations in pressure sensor readings.

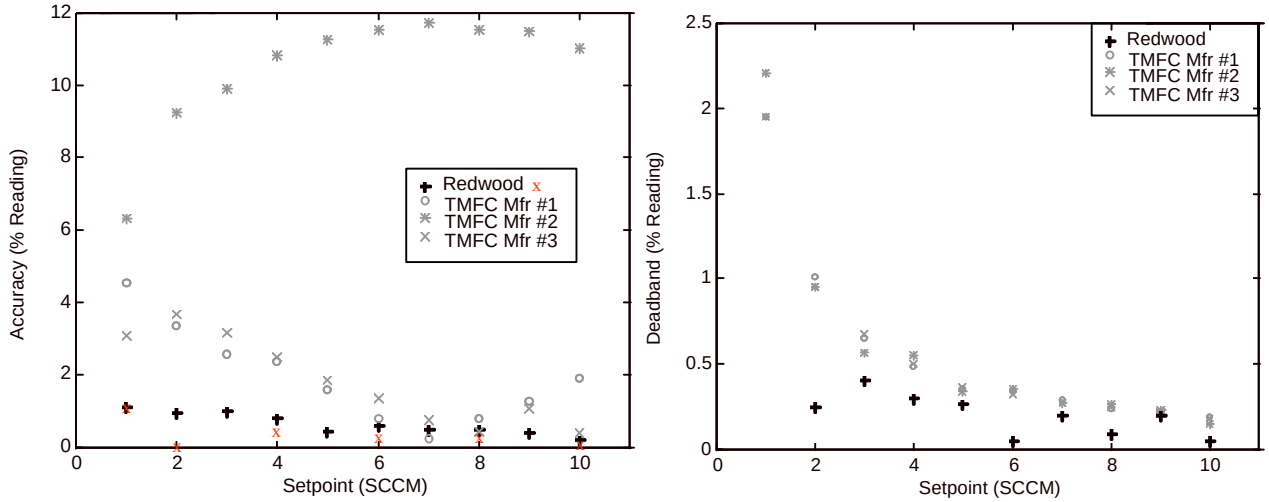

***Figure 14**: Accuracy and resolution (deadband) measurements from a 10 sccm maximum flow rate MFC, compared to measurements of MFCs from other manufacturers.*

5.0 CONCLUSIONS

We have demonstrated the science and technology required to design and fabricate flow distribution and control devices suitable for the semiconductor processing industry. Components such as pressure-based flow models, critical orifices, pressure and temperature sensors, normally-open proportional valves, and normally-closed vacuum leak rate shut-off valves, have developed. The valve actuation is based on previously developed thermopneumatic techniques. These components have been integrated into shut-off valve, mass flow controller, and pressure regulator modules, which themselves are combined at a higher level into integrated gas panels. Each integrated device has the benefit of small size, lower cost, higher resolution, materials compatibility, and lowered defect generation, which are among the attributes of the successful application of MEMS-based technology. This work has extended earlier work by providing details related to: normally-closed, vacuum leak rate shut-off valve microstructure; modeling of normally-open microvalve flow versus inlet and outlet pressure, and input power; system-level modeling of mass flow controller flow versus input power to the normally-open microvalve; and, additional measurements of mass flow controller accuracy, extending the accuracy limits to less than 0.5 percent of reading over a 10:1 dynamic range.

6.0 ACKNOWLEDGEMENTS

The efforts of Jeremy Leu and Ann-Marie Lanzillotto of David Sarnoff Research Labs, in obtaining the x-ray tomographic pictures of the vacuum leak-rate shut-off valve, are gratefully acknowledged. Some of this work was supported by DARPA under Contract #DAAL-01-94-C-3401, whose support is also acknowledged with gratitude.

7.0 REFERENCES

1. M. Zdeblick, "A planar process for an electric-to-fluidic valve." Ph.D. dissertation, Stanford University, June, 1988.
2. P. W. Barth, "Silicon microvalves for gas flow control." In Proceedings, *Transducers '95 (1995 Int'l. Conf. Sol. State Sens. and Act.)*, pp. 276-279 (IEEE, Piscataway, NJ, 1995).
3. M. Esashi, S. Eoh, T. Matsuo, and S. Choi, "The fabrication of integrated mass flow controllers." In Proceedings, *Transducers '87 (1987 Int'l. Conf. Sol. State Sens. and Act.),*, pp. 830-833 [Inst. Elec. Eng. Japan, 1987]; also, S. Shoji, B. Van der Schoot, N. de Rooij, and M. Esashi, "Smallest dead volume microvalves for integrated chemical analyzing systems." In Proceedings, *Transducers '91 (1991 Int'l. Conf. Sol. State Sens. and Act.),* pp. 1052-5 (IEEE Press, Piscataway, NJ, 1991).
4. A. K. Henning, J. Fitch, E. Falsken, D. Hopkins, L. Lilly, R. Faeth, and M. Zdeblick, "A thermopneumatically actuated microvalve for liquid expansion and proportional control." In Proceedings, *Transducers '97 (1997 Int'l. Conf. Sol. State Sens. and Act.)*, pp. 825-828 (IEEE, Piscataway, NJ, 1997).
5. J. Robertson, "An electrostatically-actuated integrated microflow controller." Ph.D. dissertation, U. Michigan, 1996.
6. A. K. Henning, "Microfluidic MEMS for semiconductor processing." In *Proceedings,2nd Annual International Conference on Innovative Systems in Silicon*, pp. 340-349 (IEEE Press, Piscataway, NJ, 1997). To appear in *IEEE Trans. Comp. Packaging and Manuf. Tech.*
7. J. S. Fitch, A. K. Henning, E. B. Arkilic, J. M. Harris, "Pressure-based mass-flow control using thermopneumatically-actuated microvalves." In *Proceedings, Solid-State Sensor and Actuator Workshop*, pp. 162-165 (Transducers Research Foundation, Cleveland, OH, 1998).
8. M. J. Zdeblick and J. B. Angell, "A microminiature electric-to-fluidic valve." In Proceedings, *Transducers '87 (1987 Int'l. Conf. Sol. State Sens. and Act.)*, pp. 827-830 (IEEE, Piscataway, NJ, 1987).
9. K. Petersen, P. Barth, J. Poydock, J. Brown, J. Mallon, Jr., and J. Bryzek, "Silicon fusion bonding for pressure sensors." In Proceedings, *IEEE Solid-State Sensor and Actuator Workshop*, pp. 144-147 (IEEE, Piscataway, NJ, 1988).
10. G. Wallis and D. I. Pomerantz, "Field-assisted glass-metal sealing." *J. Appl. Phys.* **40**, pp. 3946-3949 (1969).
11. Frank M. White, Fluid Mechanics. (McGraw-Hill, New York, 1979).
12. Mario di Giovanni, Flat and Corrugated Diaphragm Design Handbook, pp. 207-232. (Marcel Dekker, New York, 1982).
13. A. K. Henning, "Liquid and gas-liquid phase behavior in thermopneumatically actuated microvalves." To appear in Proceedings, *Micro Fluidic Devices and Systems* (International Society for Optical Engineering, Bellingham, WA, 1998; A. B. Frazier and C. H. Ahn, eds.), volume 3515.
14. E. B. Arkilic, M. A. Schmidt, and K. S. Breuer, "A technique for high resolution mass flow measurements at atmospheric pressures." *Experiments in Fluids* (in press, 1997).